Human Molecular Genetics, 2010, Vol. 19, No. 9 ***1791–1804***
doi:10.1093/hmg/ddq060
Advance Access published on February 11, 2010

AP-2α knockout mice exhibit optic cup patterning defects and failure of optic stalk morphogenesis

Erin A. Bassett[1], Trevor Williams[2,3], Amanda L. Zacharias[4,5], Philip J. Gage[4,5,6], Sabine Fuhrmann[7] and Judith A. West-Mays[1,*]

[1]Department of Pathology and Molecular Medicine, McMaster University, Hamilton, ON, Canada, [2]Department of Craniofacial Biology and [3]Department of Cell and Developmental Biology, University of Colorado Denver, Anschutz Medical Campus, Aurora, CO, USA, [4]Department of Ophthalmology and Visual Sciences, [5]Department of Cell and Developmental Biology and [6]Department of Cellular and Molecular Biology, University of Michigan Medical School, Ann Arbor, MI, USA and [7]Department of Ophthalmology and Visual Sciences, Moran Eye Center, University of Utah, Salt Lake City, UT, USA

Received January 5, 2010; Revised and Accepted February 9, 2010

Appropriate development of the retina and optic nerve requires that the forebrain-derived optic neuroepithelium undergoes a precisely coordinated sequence of patterning and morphogenetic events, processes which are highly influenced by signals from adjacent tissues. Our previous work has suggested that transcription factor activating protein-2 alpha (AP-2α; *Tcfap2a*) has a non-cell autonomous role in optic cup (OC) development; however, it remained unclear how OC abnormalities in AP-2α knockout (KO) mice arise at the morphological and molecular level. In this study, we show that patterning and morphogenetic defects in the AP-2α KO optic neuroepithelium begin at the optic vesicle stage. During subsequent OC formation, ectopic neural retina and optic stalk-like tissue replaced regions of retinal pigment epithelium. AP-2α KO eyes also displayed coloboma in the ventral retina, and a rare phenotype in which the optic stalk completely failed to extend, causing the OCs to be drawn inward to the midline. We detected evidence of increased sonic hedgehog signaling in the AP-2α KO forebrain neuroepithelium, which likely contributed to multiple aspects of the ocular phenotype, including expansion of PAX2-positive optic stalk-like tissue into the OC. Our data suggest that loss of AP-2α in multiple tissues in the craniofacial region leads to severe OC and optic stalk abnormalities by disturbing the tissue–tissue interactions required for ocular development. In view of recent data showing that mutations in human *TFAP2A* result in similar eye defects, the current findings demonstrate that AP-2α KO mice provide a valuable model for human ocular disease.

INTRODUCTION

The vertebrate forebrain is derived from a simple sheet of neuroectoderm that gives rise to complex structures of the central nervous system, including the retina and optic nerve. Patterning of the developing forebrain is influenced by surrounding tissues such as the head mesenchyme, non-neural ectoderm and ventral midline structures (1,2). As the neural tube closes, the first morphological indication of the future eye is seen as a protrusion of the forebrain called the optic vesicle (OV). As in other regions of the nervous system, regionalization of the optic neuroepithelium relies on the integration of extracellular signaling molecules and intrinsic transcriptional networks that direct the acquisition of neuronal, glial or epithelial phenotypes. As the OV invaginates to form a bilayered optic cup (OC), it becomes partitioned into three domains: the neural retina (NR), retinal pigment epithelium (RPE) and optic stalk. These patterning events are highly dependent upon signaling interactions with the periocular mesenchyme (POM), a loosely aggregated population of mesenchymal cells that surrounds the developing eye and contributes to multiple ocular structures (3), the surface ectoderm, which generates the lens and cornea and is in close contact with the distal OV during lens placode formation (4), as well as adjacent neuroepithelial tissue (5).

*To whom correspondence should be addressed at: Department of Pathology and Molecular Medicine, McMaster University, Health Sciences Centre, Room 1R10, Hamilton, ON, Canada L8N 3Z5. Tel: +1 9055259140; Fax: +1 9055257400; Email: westmayj@mcmaster.ca

Multiple studies in chick, fish and mouse models have shown that midline-derived sonic hedgehog (SHH) provides essential cues to the developing optic neuroepithelium (6–9). Fibroblast growth factor (FGF) signals from the ocular surface ectoderm have an organizational role in patterning the OV, by promoting NR formation and repressing RPE specification (10–12). Studies using explant cultures of chick OVs have shown that a transforming growth factor beta-like signal from the POM favors RPE formation through induction and maintenance of RPE-specific genes and inhibition of NR-specific transcription factors (13). Differentiation of the POM is intrinsically regulated by transcription factors such as FOXC1 and PITX2 (14,15), and also influenced by signals from the lens and OC (16,17). As well as being crucial for the development of POM-derived structures of the eye, transcription factors expressed in the POM can also have non-cell autonomous influences on additional ocular tissues, as has been demonstrated for PITX2 in optic stalk morphogenesis (15). Components of the bone morphogenetic protein (BMP), retinoic acid (RA) and Wnt signaling pathways are also expressed in ocular and periocular regions, and there is increasing evidence for the involvement of these pathways in specification of the optic neuroepithelium (5,17–22).

Mutations in the human transcription factor activating protein-2 alpha (AP-2α) gene, *TFAP2A*, have recently been shown to cause Branchio-oculo-facial syndrome (BOFS) (23–26), an autosomal dominant disorder characterized by craniofacial and eye defects (27,28). Our previous work has established AP-2α as a crucial regulator of ocular morphogenesis (29–34). During mouse eye development, AP-2α, encoded by *Tcfap2a*, is expressed in ocular and periocular tissues, including the lens placode and its derivatives, the POM and the NR (29,34). *Tcfap2a* germ-line knockout (KO) mice have eyes embedded inside the head that exhibit absent cornea and eyelids, failed or defective lens induction and abnormalities in the OC. Though no AP-2 proteins are expressed in the RPE, lamination defects in the inner NR are accompanied by a striking OC patterning defect, in which a variable portion of the RPE is converted to an inverted NR (29,34). Our subsequent studies of lens placode-specific *Tcfap2a* KOs demonstrated an intrinsic role for AP-2α in lens vesicle separation and maintenance of the lens and corneal epithelial cell phenotypes, and also revealed that confining the *Tcfap2a* deletion exclusively to the developing lens did not impact NR or RPE development (32,33). In addition, we recently showed that conditional deletion of *Tcfap2a* in the developing retina did not lead to any OC defects observed in *Tcfap2a* germ-line KOs (34). These outcomes have prompted us to re-examine the OC phenotype in *Tcfap2a* germ-line KOs (referred to herein as AP-2α KOs), and consider the non-cell autonomous roles for AP-2α in OV/OC development and specification or maintenance of the RPE. Our findings show that overall craniofacial dysgenesis in the germ-line KOs, resulting from loss of *Tcfap2a* in multiple tissues, disturbs the tissue–tissue interactions required for OC and optic stalk development.

RESULTS

Expression pattern of AP-2α during OC development

Although we have previously reported on AP-2α expression in the developing lens and retina, we have not followed its expression pattern in the early embryonic ocular region, particularly in the head mesenchyme cells surrounding the eye. Although AP-2α is known to be expressed in the neural crest-derived head mesenchyme (35–38), its expression pattern specifically in the POM has not been examined. Our current analysis shows that, as expected, AP-2α protein was expressed in the surface ectoderm throughout OC formation, and remained in the anterior lens epithelium following its separation from the surface ectoderm (Fig. 1). At embryonic day (E) 8.75, when the OV is evaginating but has not yet reached the surface ectoderm, the majority of head mesenchyme cells surrounding the early OV expressed AP-2α (Fig. 1A). By E9.5, AP-2α was detected in a small population of POM cells adjacent to the RPE domain in the dorsal OV (Fig. 1B), which is the region of optic neuroepithelium containing presumptive RPE cells that eventually occupy the outer layer of the OC. AP-2α was not detected in the POM beyond E10.5, and was absent from neuroepithelial-derived ocular structures until later stages of OC morphogenesis, when it is expressed in developing amacrine cells of the NR (Fig. 1C–E and not shown; 34).

Defects in AP-2α KO optic neuroepithelium begin at OV stage

We have previously shown that the OCs in AP-2α KOs become embedded inside the head and exhibit a variable defect in which a portion of the RPE is replaced by a duplicated, inverted NR (29,34). However, it remained unclear how these defects developed at the morphological and molecular level. To this end, we first conducted a detailed histological examination of the AP-2α KO ocular region during OC development (Figs 2 and 3). Compared with control littermates, in which there was a clear demarcation between the telencephalic and diencephalic vesicles by E9.5 (Fig. 2A), the anterior neural tube in AP-2α KOs remained a single narrow vesicle and failed to close (Fig. 2 E and F, red asterisks). By E9.5, it was apparent that OVs evaginated from the forebrain of AP-2α KOs, but were mispositioned (Fig. 2E). In contrast to control littermates, the distal portion of the OV (future NR) in AP-2α KOs failed to orient itself correctly with respect to the surface ectoderm and instead predominantly faced POM (Fig. 3A and E, red asterisks). By E10.5 during normal mouse embryogenesis, the developing RPE is a 1–2 cell thick layer in the outer OC, and the optic stalk has begun to thin and elongate as the space between the OC and diencephalon expands (Fig. 2B). In contrast, the optic stalk in AP-2α KOs remained thicker and failed to lengthen in the same fashion as controls (Fig. 2B and F, red arrowheads). The AP-2α KO OVs invaginated to form OCs with an outer layer that appeared similar in thickness to the wild-type presumptive RPE (Fig. 3B and F, black arrows); however, the proximal-most region adjacent to the optic stalk was consistently thickened compared with controls (Fig. 3B and F, orange arrowheads). At this stage, morphogenesis of the AP-2α KO ventral retina appeared delayed compared with controls (Fig. 3B and F, bottom orange arrowheads). By E11.5, the AP-2α KO OCs were connected to the neural tube by a shortened, thickened optic stalk (Fig. 2G, red arrowheads), and were often severely turned, at times as much as

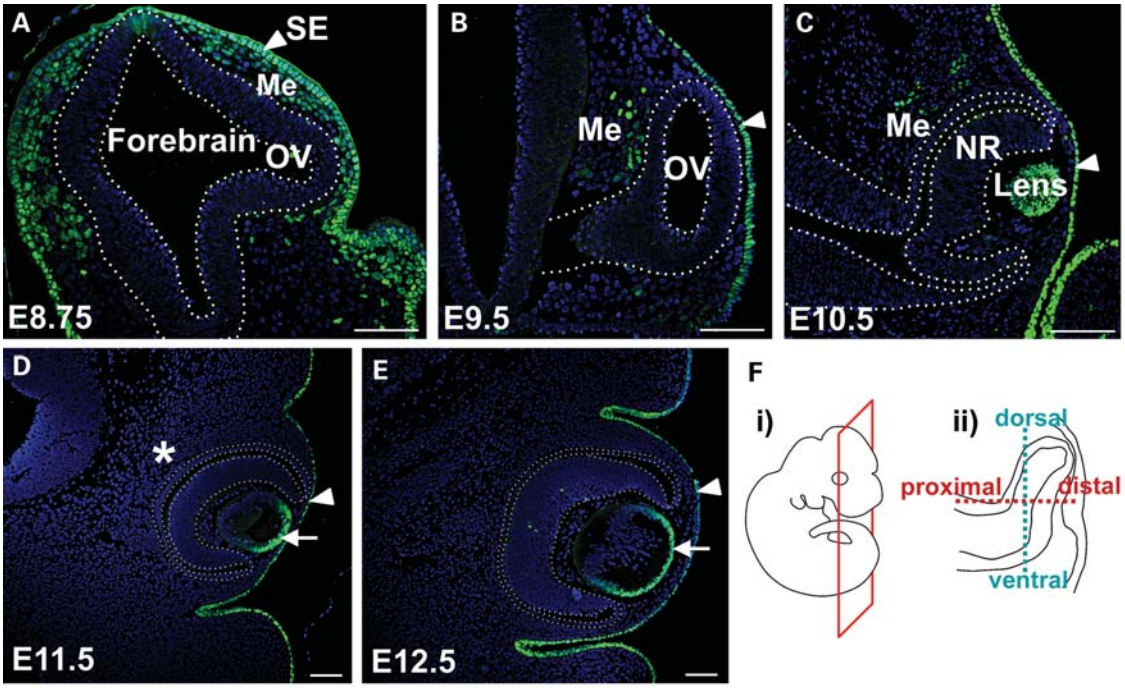

Figure 1. Expression pattern of AP-2α protein during early eye development. Immunofluorescence using an anti-AP-2α antibody (green) on sections of wild-type embryos counterstained with DAPI (blue). (**A**–**E**) Coronal paraffin sections of mouse embryo heads at the developmental stages indicated. Outlined region in A indicates the forebrain neuroepithelium, including an evaginating OV. Outlined regions in B–E demarcate the OV/OC. Arrowheads in A–E denote surface ectoderm, whereas arrows in D, E denote anterior lens epithelium. AP-2α was not detected in the periocular mesenchyme beyond E10.5 (asterisk in D). (**F**) Schematics showing the plane of section (i) used on all embryos throughout this study except for sagittal sections in Fig. 7, and the dorsal-ventral and proximal-distal axes in the developing optic neuroepithelium (ii). SE, surface ectoderm; OV, optic vesicle; Me, mesenchyme; NR, neural retina. Scalebars, 100 μm.

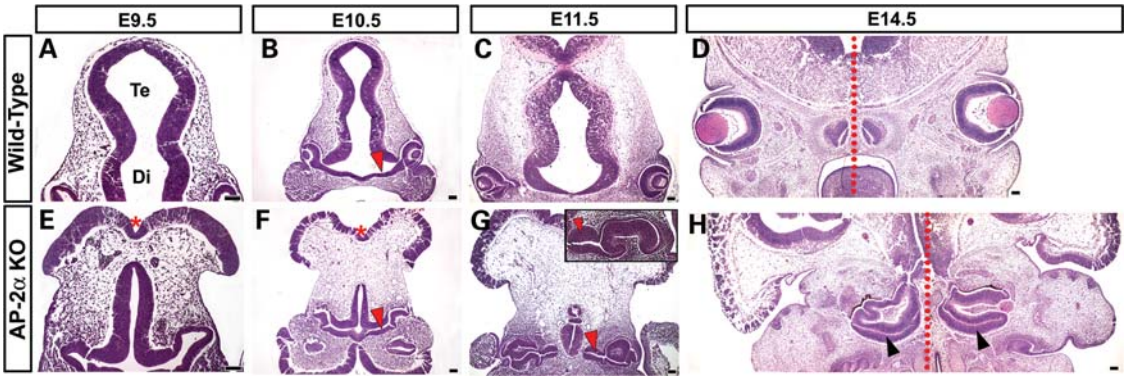

Figure 2. Defects in AP-2α KO cranial and ocular regions arise during early eye morphogenesis. (**A**–**H**) Coronal H&E-stained paraffin sections of wild-type (A–D) and AP-2α KO (E–H) embryo heads at the stages indicated. Red asterisks (E, F) denote the open cranial neural tube in AP-2α KO mice. Red arrowheads (B, F, G) show the shortened, thickened optic stalk in AP-2α KOs compared with controls. Inset in G illustrates example of a severely turned AP-2α KO eye. By E14.5, the AP-2α KO eyes are adjacent to the midline (dotted red lines in D, H). Black arrowheads (H) show duplicated NR in the ventral AP-2α KO OC. Te, telencephalon; Di, diencephalon. Scalebars, 100 μm.

90° relative to the surface ectoderm compared with controls (see eyes in Fig. 2C versus G, inset). This turning was often associated with mispositioning of the mutant lens. Regions of the outer OC layer were visibly thickened (Fig. 3G, arrowheads) compared with the presumptive RPE of controls, which had formed a monolayer by this stage (Fig. 3C, arrow). At E11.5 and onwards, we commonly observed eyes in which at least half of the outer OC had a duplicated NR forming in place of the RPE (Figs 2H and 3G, H). In the AP-2α KOs, the ventral retina either remained underdeveloped (Fig. 3I and J, red arrows), or did undergo morphogenesis to a variable degree but displayed a duplicated NR in the outer OC (Figs 2H and 3G, H, black arrowheads). We also observed thickening in regions of the dorsal presumptive RPE (Fig. 3G–J, blue arrowheads). Beyond E12.5, the AP-2α KO OCs became further buried inside the head such that an optic stalk remnant was virtually absent, and the eyes were directly attached to the poorly developed neural tube (Fig. 2H). Multiple aspects of the AP-2α KO ocular phenotype were variable, including the extent of RPE-to-NR conversion, the

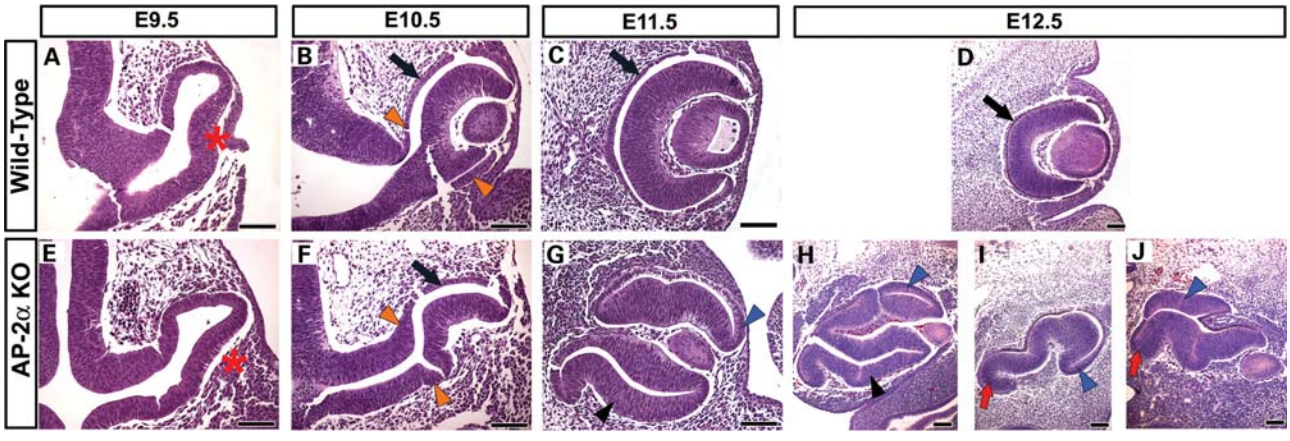

Figure 3. AP-2α KO eye defects begin at OV stage. (**A**–**J**) Coronal H&E-stained paraffin sections of wild-type (A–D) and AP-2α KO (E–J) embryo heads at the stages indicated. (A, E) Red asterisks denote the mispositioning of the AP-2α KO OV at E9.5, which was not oriented correctly with respect to the surface ectoderm. (B, F) Black arrows point to regions of the wild-type and AP-2α KO outer OC that are similar in thickness, whereas orange arrowheads point to regions of presumptive RPE adjacent to the optic stalk that are thickened in AP-2α KOs compared with controls. (C, D, G–J) Although the RPE formed a clear monolayer at E11.5 and onwards in wild-type eyes (black arrows in C, D), regions of the outer OC layer in AP-2α KOs were visibly thickened in both the dorsal OC (blue arrowheads in G–J) and ventral OC (black arrowheads in G, H). Red arrows in I, J show AP-2α KO eyes with an underdeveloped ventral retina. Scalebars, 100 μm.

presence of an obvious lens (which occurred in 75% of AP-2α KO eyes examined) and degree of eye turning.

Patterning and lamination defects in AP-2α KO NR

To assess how the abnormal ocular morphology in AP-2α KOs impacted OV/OC patterning, we examined the expression of patterning markers by immunofluorescence. These included VSX2 (formerly CHX10), the earliest marker of the presumptive NR and MITF, which is initially expressed throughout the entire mouse OV and becomes restricted to the presumptive RPE by E9.5 (12,39–41). At E9.5 and E10.5, although VSX2 protein in the AP-2α KO was detected in the correct region (presumptive NR), its expression appeared reduced compared with controls (Fig. 4A, B, E, F, arrows). This was accompanied by persistence of MITF as well as the RPE determinant OTX2 (42) in the NR territory (Fig. 4M and N, arrows and not shown), both of which were already down-regulated in this region in controls (Fig. 4I and J and not shown). Interestingly, by E11.5 the AP-2α KO NR no longer misexpressed MITF or OTX2 (Fig. 4O and not shown) and expressed VSX2 in a pattern that resembled the control NR (Fig. 4C and G). Throughout embryogenesis, PAX6 expression in the developing AP-2α KO NR did not differ from wild-type littermates (not shown). In addition to NR progenitor factors (PAX6 and VSX2), indicators of retinal neurogenesis were also detected in the AP-2α KO. An anti-ISL1/2 (Islet-1/2) antibody, which labels developing amacrine and ganglion cells at E14.5 (43,44), showed similar expression patterns in the AP-2α KO and control NR, primarily in the inner retina with a few positive cells scattered in the outer neuroblast layer (Supplementary Material, Fig. S1A and D). These data confirm our previous finding that early neurogenesis was largely unaffected in the AP-2α KO NR (34). However, by late embryogenesis, we observed a general deterioration of NR architecture in AP-2α KOs, as lamination failed to progress and the cells appeared increasingly disorganized compared with controls (Supplementary Material, Fig. S1B and E).

Conversion of AP-2α KO RPE to a second NR

The expression patterns of genes in the presumptive RPE domain were also altered in AP-2α KOs. Both *Mitf* and *Otx2* are key upstream regulators of the genetic cascades that confer pigmented epithelial properties to the RPE (21). At OV and early OC stages, MITF and OTX2 were expressed in the developing RPE territory in wild-type and AP-2α KO eyes (Fig. 4I, J, M, N, arrowheads and not shown). However, by E11.5 and onwards, when the duplicated NR was clearly evident, MITF and OTX2 protein expression was either not detected or reduced in thickened regions of presumptive RPE (Fig. 4O and P, white outlines and not shown). The absence of RPE-promoting genes was accompanied by ectopic VSX2 expression in the outer layer of the OC (Fig. 4G and H, outlined regions) as well as an increase in phospho-histone H3 (PH3)-labeled cells (Fig. 9F). Whereas the loss of RPE characteristics consistently occurred throughout the entire ventral OC, this phenomenon was more patchy in the dorsal OC—although it was commonly observed in the distal-most presumptive RPE facing the surface ectoderm (Fig. 4G, H, O, P). As we have previously reported (34), the duplicated NR also expressed markers of neurogenesis in a temporally similar fashion as the primary NR, though in an inverted orientation. These included indicators of retinal ganglion cells (RGCs)-POU4F2 (BRN3B), ISL1/2, CALB2 (calretinin), as well as amacrine cells-ISL1, CALB2 [Supplementary Material, Fig. S1A, B, D, E and not shown (34)]. We also examined the expression of OTX2 in the duplicated NR during late embryogenesis. In addition to promoting RPE specification, OTX2 is expressed in post-mitotic retinal neuroblasts and is known to be required for mouse photoreceptor and bipolar cell development (45–47).

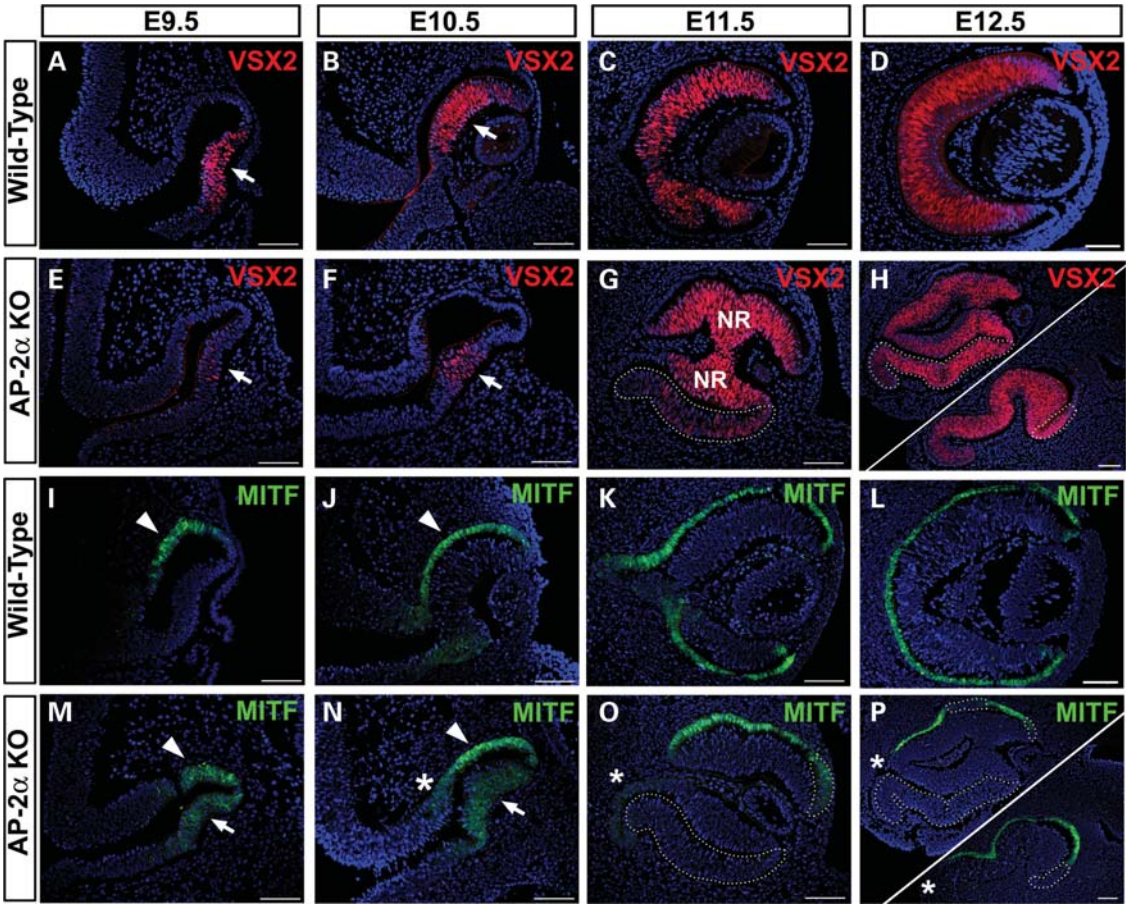

Figure 4. Ocular patterning defects and formation of a duplicated NR in AP-2α KOs. Immunofluorescence using anti-VSX2/CHX10 (red) and anti-MITF (green) on coronal sections of wild-type (**A**–**D**, **I**–**L**) and AP-2α KO (**E**–**H**, **M**–**P**) embryo heads counterstained with DAPI (blue), at the stages indicated. Examples of two E12.5 eyes are shown (H, P), to illustrate the variability in the extent and location of ectopic NR tissue. (A, B, E, F) Arrows point to VSX2 expression in NR domain, which was reduced in AP-2α KOs compared with controls at E9.5 and E10.5. (I, J, M, N) Arrowheads denote MITF expression in the wild-type and AP-2α KO RPE domain, whereas arrows point to persistent MITF expression in the NR domain of AP-2α KOs at E9.5 and E10.5. (C, D, G, H) Outlined regions illustrate ectopic VSX2 expression in the AP-2α KO duplicated NR. (K, L, O, P) Outlined regions show absent or reduced MITF expression in thickened regions of the AP-2α KO outer OC. Asterisks (N–P) indicate additional regions of the outer OC adjacent to the midline that lack MITF expression. Scalebars, 100 μm.

At E17.5, OTX2 expression in the NR is concentrated in the outer neuroblast layer containing the presumptive photoreceptors (47). An inverted version of this expression pattern was also detected in the AP-2α KO duplicated NR, providing evidence of photoreceptor specification in the normal and ectopic retina (Supplementary Material, Fig. S1C and F).

Expansion of Pax2 into the AP-2α KO presumptive RPE territory

Beginning at E10.5, we noted an additional region of the AP-2α KO outer OC at the OC-optic stalk border that did not exhibit an RPE phenotype (Fig. 4N, asterisk). A section of presumptive RPE adjacent to the midline showed reduced or absent MITF and OTX2 expression compared with controls (Fig. 4N–P, asterisks and not shown), and also lacked PAX6 expression by E11.5 and onwards (not shown). Immunostaining of adjacent sections with anti-PAX2 showed that this region corresponded to a portion of the presumptive RPE in which PAX2 was ectopically expressed (Fig. 5 and not shown). The lack of PAX6 expression in this region was not unexpected, given that reciprocal inhibition between PAX6 and PAX2 is involved in establishing the OC versus optic stalk territories (48). During eye morphogenesis PAX2 is expressed primarily in the ventral OV and later becomes restricted to the optic fissure and optic stalk (49,50). Further examination of PAX2 expression showed that whereas it was largely confined to the ventral NR and ventral optic stalk domains in wild-type eyes at E9.5 and E10.5, it appeared to be expanded dorsally in AP-2α KOs (Fig. 5A, B, F, G, arrowheads). The portion of outer OC into which PAX2 had expanded corresponded to the consistently thickened region of presumptive RPE adjacent to the optic stalk noted during histological examinations (compare Figs 3F and 5G). Between E11.5 and E14.5, PAX2 gradually became confined to the optic stalk and newly formed optic disk in wild-type embryos (Fig. 5C–E). In AP-2α KOs, the shortened PAX2-postitive optic stalk seen at E11.5 (Fig. 5H) was nearly absent by E12.5, in which only a small remnant of PAX2-positive optic stalk that was attached almost directly to the neural tube could be detected (not shown). Beginning at E11.5, the PAX2 expression domain in AP-2α KOs was clearly extended into regions of presumptive

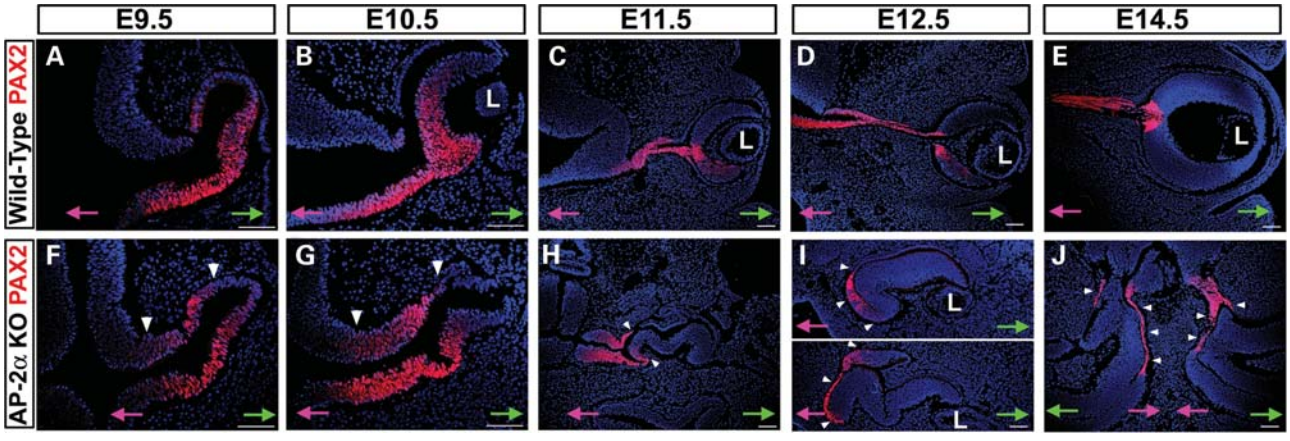

Figure 5. PAX2 expansion into RPE domain in AP-2α KOs. Immunofluorescence using anti-PAX2 (red) on coronal sections of wild-type (**A**–**E**) and AP-2α KO (**F**–**J**) embryo heads counterstained with DAPI (blue), at the stages indicated. (A, B, F, G) White arrowheads show dorsal expansion of PAX2 expression in AP-2α KO eyes compared with wild-type eyes at E9.5 and E10.5. (C–E, H–J) Although PAX2 became confined to the optic stalk and newly formed optic disk in wild-type embryos, white arrowheads denote expansion of the PAX2 expression domain into regions of presumptive RPE closest to the midline in AP-2α KOs. Refer to Fig. 2H for an H&E stain of the same embryo depicted in J. Pink and green arrows in A–J point towards midline and surface ectoderm, respectively. L, lens. Scalebars, 100 μm.

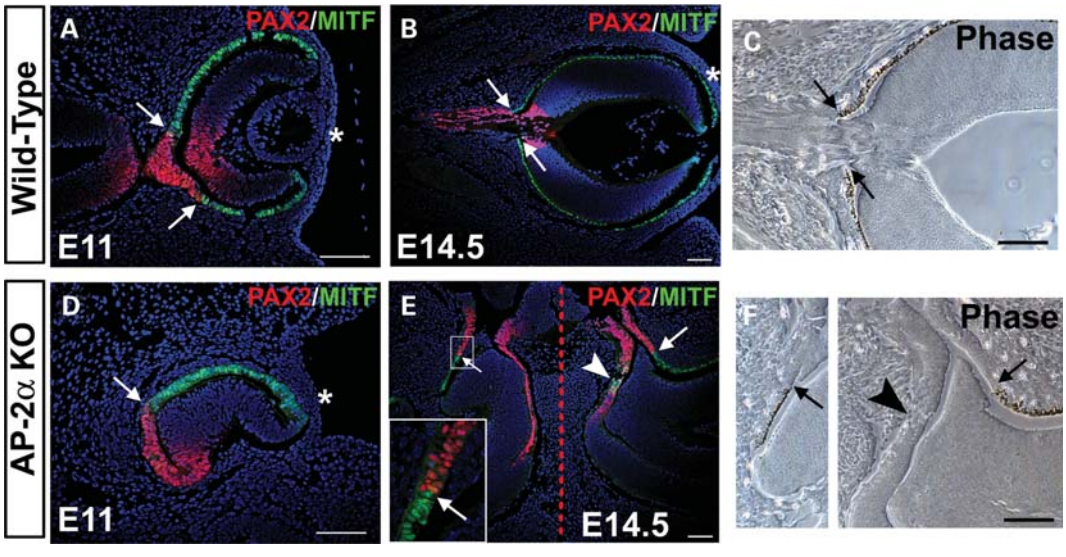

Figure 6. The PAX2-MITF border is shifted into the OC in AP-2α KOs. (**A**, **B**, **D**, **E**) Co-immunostaining of PAX2 (red) and MITF (green) on coronal sections of wild-type (A, B) and AP-2α KO (D, E) embryo heads counterstained with DAPI (blue), at the stages indicated. White arrows (A, B, D, E) denote the PAX2-MITF borders, whereas white arrowhead (E) indicates overlap of PAX2-positive and MITF-positive cells. Asterisks (A, B, D) mark the surface ectoderm. Dashed red line (E) marks the midline. Boxed area in E is magnified in inset. (**C**, **F**) Corresponding phase views of the eyes in B and E, respectively. Black arrows point to the border between pigmented versus non-pigmented cells, and black arrowhead denotes lack of pigmentation in area of PAX2-MITF overlap. Refer to Fig. 2H for an H&E stain of the same embryo depicted in E and F. Scalebars, 100 μm.

RPE closest to the neural tube (Fig. 5H–J, arrowheads). During OC morphogenesis, the reciprocal expression patterns of PAX2 and MITF demarcate a tight RPE-optic stalk boundary (Fig. 6A, arrows) in which PAX2-positive cells do not overlap with MITF-positive pigmented cells of the presumptive RPE (51; Fig. 6B and C, arrows). Co-staining of PAX2 and MITF in AP-2α KO embryos at multiple stages of OC development (E11, 11.5, 12.5 and 14.5) revealed that regions of the presumptive RPE ectopically expressing PAX2 were almost always MITF-negative, so that the border between PAX2-positive and MITF-positive cells was maintained but 'shifted' into the OC (Fig. 6D and E, arrows). Corresponding phase views at E14.5 showed that sharp MITF-PAX2 borders were associated with pigmented versus non-pigmented cells in both wild-type and AP-2α KOs (Fig. 6B, C, E, F, arrows). However, unlike wild-type eyes, occasional intermingling of PAX2-positive and MITF-positive cells was detected in AP-2α KOs (Fig. 6E, arrowhead). Closer inspection showed that PAX2-MITF overlap in AP-2α KOs was found only in non-pigmented regions (Fig. 6F, arrowhead).

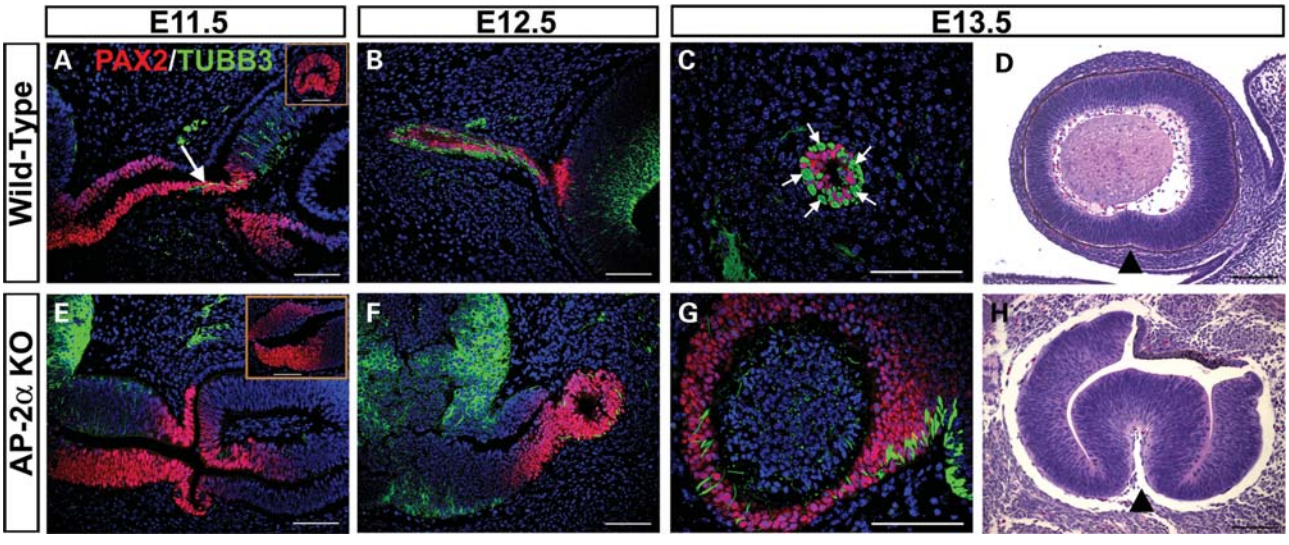

Figure 7. Optic nerve development and optic fissure closure are impaired in AP-2α KOs. (**A**–**C**, **E**–**G**) Co-immunostaining of PAX2 (red) and neuron specific class III β-tubulin (TUBB3; green) on coronal (A, B, E, F) and sagittal (C, G) sections of wild-type (A–C) and AP-2α KO (E–G) embryo heads counterstained with DAPI (blue), at the stages indicated. Arrow (A) points to TUBB3-positive RGC axons entering the PAX2-positive optic stalk and extending towards the diencephalon, which was not observed in AP-2α KOs (E, F). Insets (A, E) show view of PAX2-stained optic stalk from sagittal sections of wild-type (A) or AP-2α KO (E) embryos at E11.5. Arrows in C show examples of TUBB3-positive RGC axon bundles adjacent to PAX2-positive glial precursors in the wild-type E13.5 optic stalk. (**D**, **H**) Sagittal H&E-stained sections of AP-2α KO and control littermate embryo heads. By E13.5, the optic fissure margins in wild-type eyes had fully fused along the ventral OC, but were consistently open in AP-2α KOs (black arrowheads). Scalebars, 100 μm.

Optic nerve development and optic fissure closure are impaired in AP-2α KOs

Our histological observations of AP-2α KO eyes showed that optic nerve morphogenesis was defective (Fig. 2). Expression of PAX2 in the early AP-2α KO optic stalk (Fig. 5F–H) suggested correct patterning of cells in this region; however, optic stalk dysgenesis was evident as early as E10.5 (Figs 2F and 5G). At E11.5 in wild-type embryos, the first RGC axons entered the PAX2-positive optic stalk, as detected by double immunostains for neuron specific class III β-tubulin (TUBB3) and PAX2 (Fig. 7A, arrow). By E12.5, wild-type RGC axons were interspersed among PAX2-positive optic stalk cells (Fig. 7B), which are glial precursors that will mature as astrocytes of the optic nerve (50). By E13.5, a sagittal embryo section including the wild-type optic stalk showed bundles of RGC axons adjacent to PAX2-positive glial precursors (Fig. 7C, arrows). In contrast, though we detected BRN3B-positive RGCs in AP-2α KOs throughout embryogenesis (not shown), we failed to observe RGC axons exiting the eye and extending towards the diencephalon, nor did we detect an appreciable intermingling of TUBB3-positive and PAX2-positive cells in the optic stalk region (Fig. 7E and F). By E13.5, attempts to obtain sections of an AP-2α KO optic stalk revealed a region that had failed to condense into an optic nerve-like structure, with PAX2-positive cells concentrated towards the outer margins (Fig. 7G). Sagittal sections of AP-2α KO and control littermate embryos confirmed a lack of optic fissure closure in mutant embryos (Fig. 7D and H). In the mouse, closure of the optic fissure begins at E11 and is complete by E13 (52). By E13.5, the optic fissure margins in wild-type eyes had fully fused along the ventral OC, but were consistently open in AP-2α KOs (Fig. 7D and H, arrowheads), a phenotype that persisted until the latest AP-2α KO stage examined, E17.5 (not shown).

Altered gene expression in AP-2α KO ocular region

SHH secreted from ventral midline structures is required for morphogenesis and patterning of the optic neuroepithelium (5). We therefore used *in situ* hybridization to investigate the expression pattern of *Gli1*, a direct target of the SHH pathway that provides a readout of SHH signaling (53,54). At E9.5, *Gli1* transcripts are detected in the OV and regions of the neural tube close to the source of SHH (55,56; Fig. 8A). In three of four AP-2α KO embryos examined at the OV stage, the hybridization signal for *Gli1* in regions of the forebrain neuroepithelium and proximal OV was increased compared with wild-type littermates (Fig. 8E, arrows), suggestive of altered SHH responsiveness in the AP-2α KO neural tube. To extend this analysis, we examined the protein expression of ISL1, a marker of ventral forebrain neurons that is induced by SHH (57) and ectopically expressed in the neural tube of mouse mutants with increased activation of the SHH pathway (58,59). Using anti-ISL1/2 antiserum on E10.5 (Fig. 8B and F) and E11.5 (not shown) frontal sections at the level of the eyes, ISL1-positive cells were detected in distinct areas of the wild-type forebrain adjacent to known sources of SHH (60; Fig. 8B, red arrows). In contrast, ISL1-positive cells were detected throughout the neural tube in the ocular region of AP-2α KOs (Fig. 8F), supporting the fact that SHH-related patterning of the forebrain neuroepithelium is perturbed.

Given that the POM provides extrinsic cues to the optic neuroepithelium (13,15), we also considered the possibility that POM-related development may be affected in the AP-2α KO

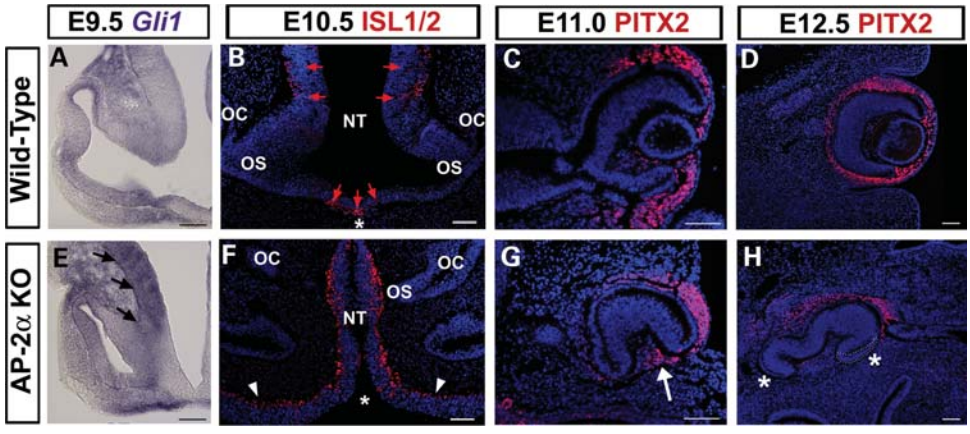

Figure 8. Altered gene expression in neural tube and POM of AP-2α KOs. (**A**, **E**) *In situ* hybridization of *Gli1* (purple) on coronal sections of wild-type (A) and AP-2α KO (E) embryo heads at E9.5. Black arrows in E indicate increased signal in AP-2α KO neural tube and proximal OV. (**B**–**D**, **F**–**H**) Immunofluorescence using anti-ISL1/2 (B, F) and anti-PITX2 (C, D, G, H) (red) on coronal sections of wild-type (B–D) and AP-2α KO (F–H) embryo heads counterstained with DAPI (blue), at the stages indicated. Asterisks in B and F indicate the closed versus open neural tube in wild-type and AP-2α KO, respectively. Red arrows in B show ISL1-positive cells in wild-type forebrain. Arrowheads in F denote overgrown neuroepithelium in AP-2α KO. Arrow in G indicates PITX2-positive cells inside the AP-2α KO OC at E11. Asterisks in H denote regions adjacent to the mutant OC that contain either fewer or no cells expressing PITX2. Outlined area in H indicates ectopic NR. OS, optic stalk; OC, optic cup; NT, neural tube. Scalebars, 100 μm.

eye phenotype. We examined the expression of *Pitx2*, a homeobox gene crucial for the development of both POM-derived and non-POM-derived ocular tissues (15,61,62). At E11, PITX2 protein was detected in both the wild-type and AP-2α KO periocular region (Fig. 8C and G). By E11.5 during normal mouse development, a small population of POM cells invade the hyaloid space between the posterior lens and retina to form the hyaloid vasculature (3). However, presumably due to the absent or defective lens, PITX2-positive cells were detected inside the AP-2α KO OC at E11, in the space that would normally be occupied by a full-size lens vesicle (Fig. 8G, arrow). In addition, the turning of the AP-2α KO eyes further disrupted their positioning with respect to the POM, such that only a portion of the OC was surrounded by PITX2-expressing cells (Fig. 8, compare C with G). This phenomenon was more apparent by E12.5, at which time there also appeared to be a slight reduction in periocular PITX2 expression compared with control littermates (Fig. 8, compare D with H). Although wild-type eyes were extensively surrounded by PITX2-positive cells, regions of AP-2α KO eyes were adjacent to either fewer, or no, cells expressing PITX2 (Fig. 8H, asterisks). In the samples examined, areas of the POM with loss of PITX2 expression were associated with regions of the AP-2α KO OC containing ectopic NR (Fig. 8H, white outline and not shown).

Abnormal patterns of proliferation and programmed cell death in AP-2α KO eyes

We examined cell proliferation (via PH3 expression) and apoptosis (via TUNEL assays) in AP-2α KO eyes during OC formation. As expected, regions of the AP-2α KO outer OC showed increased PH3 labeling compared with the corresponding areas in wild-type controls. These included the region at the optic stalk-RPE border that was notably thicker in AP-2α KOs at E10.5 (Fig. 9A and E, brackets), as well as the duplicated NR evident in AP-2α KOs by E11.5 (Fig. 9F, arrows). TUNEL analysis of AP-2α KOs during and after OC formation revealed two consistent alterations in the distribution of apoptotic cells. Firstly, during early OC invagination at E10.0, wild-type controls exhibited a zone of cell death known to occur in the ventral optic neuroepithelium (Fig. 9C, asterisk; 63–65), whereas an absence of TUNEL labeling showed that this apoptotic zone was not detected in AP-2α KOs (Fig. 9G, asterisk). Secondly, E11.5 AP-2α KOs lacked the extensive TUNEL-positive cells observed in the ventral wall of the optic stalk in controls (Fig. 9D and H, solid arrowheads; 63,66). We also noted that following OC morphogenesis, four of the six AP-2α KO eyes examined at E11.5 showed increased TUNEL labeling in the OC compared with controls (Fig. 9H and inset, open arrowheads). Aside from these observations, we did not detect any consistent differences in TUNEL labeling between AP-2α KOs and wild-type littermates within the eye or surrounding POM.

DISCUSSION

Throughout eye development, specification and differentiation of neuroectoderm-derived tissues involves precisely coordinated tissue–tissue interactions. We have shown that while AP-2α is not expressed in the early optic neuroepithelium, germ-line deletion of *Tcfap2a* affects the morphogenesis and patterning of this tissue in a non-cell autonomous fashion.

OC and optic stalk defects in AP-2α KOs are associated with abnormalities in multiple tissues

Our observations in this study, combined with those of tissue-specific AP-2α KO mice, show that impaired development of the AP-2α KO optic neuroepithelium is not a cell autonomous phenomenon, but rather a result of gross morphological defects caused by loss of *Tcfap2a* in multiple surrounding tissues. Previous reports from our laboratory have shown

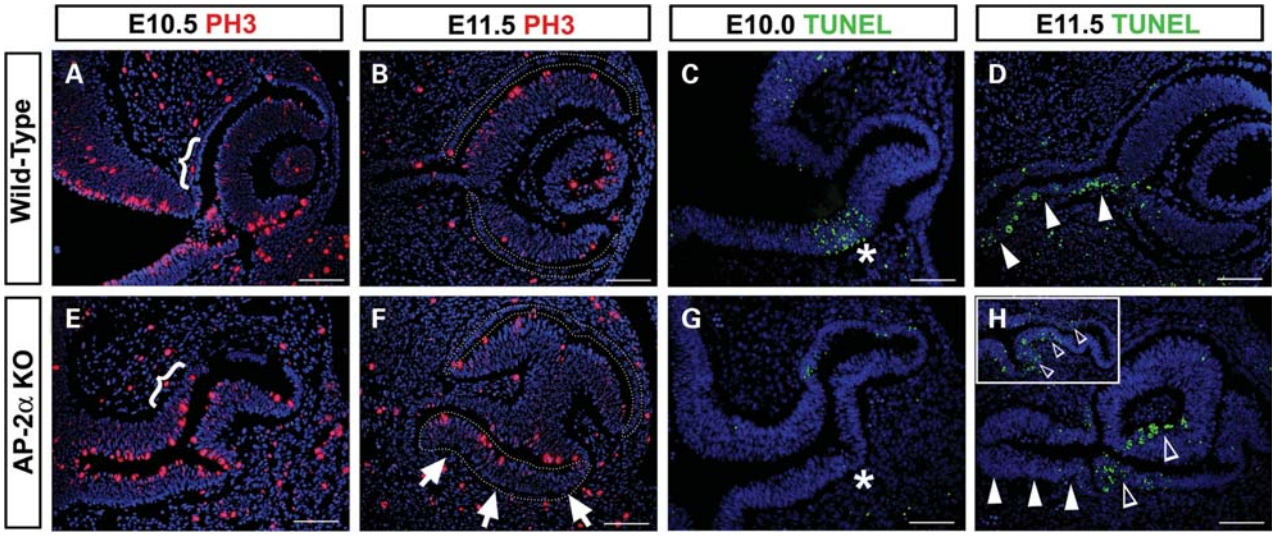

Figure 9. Changes in cell proliferation and apoptosis in AP-2α KO eyes. (**A**, **B**, **E**, **F**) Immunofluorescence using the mitotic marker PH3 (red) on coronal sections of wild-type (A, B) and AP-2α KO (E, F) embryo heads counterstained with DAPI (blue), at the stages indicated. Brackets (A, E) indicate the region at the optic stalk-RPE border in which AP-2α KOs show an increase in PH3-labeled cells compared with controls. Outlines (B, F) denote the presumptive RPE territory, and arrows in F point to a highly proliferative area in the AP-2α KO outer OC. (**C**, **D**, **G**, **H**) Apoptotic cells (green) detected using the TUNEL assay on coronal sections of wild-type (C, D) and AP-2α KO (G, H) embryo heads counterstained with DAPI (blue), at the stages indicated. Asterisks (C, G) indicate the previously reported ventral region of apoptosis (C), which was not detected in AP-2α KOs (G). Solid arrowheads (D, H) point to the E11.5 optic stalk, in which AP-2α KOs lacked the apoptotic cells seen in wild-type eyes. Inset in H shows example of a second AP-2α KO OC at E11.5. Open arrowheads (H) show examples of cells undergoing programmed death in the AP-2α KO OCs. Scalebars, 100 μm.

that AP-2α is expressed in the developing lens and later in the developing OC, specifically in amacrine cells, yet deletion of *Tcfap2a* from the lens placode (32) or OC (34) did not lead to defects in any derivatives of the optic neuroepithelium. However, germ-line deletion of *Tcfap2a* causes extensive defects in morphogenesis and patterning of the OC and optic stalk. In this study, we have shown that AP-2α is expressed in the POM surrounding the early OV (Fig. 1). The neural crest, which is a major contributor to the mesenchyme in the craniofacial and ocular regions (3,67), is well-established as a site of AP-2α expression and function. Thus, involvement of the AP-2α-expressing neural crest-derived POM in development of the OV is an intriguing possibility. However, it has been shown that neural crest-specific deletion of *Tcfap2a* using Wnt1-Cre transgenic mice (68) does not cause obvious morphological eye defects by E15.5 (T.W. and E.B., unpublished observations), demonstrating that loss of AP-2α in the neural crest alone is not sufficient to generate an ocular phenotype resembling that of AP-2α germ-line KOs. At E8.0, *Tcfap2a* expression is initially detected in the non-neural ectoderm and presumptive neural crest cells at the neural plate border (69), but is not expressed in the neural plate proper or in the forebrain neuroepithelium during OV evagination. Taken together, these data suggest that deletion of *Tcfap2a* in multiple ectodermal derivatives has non-cell autonomous effects on development of the OC and optic stalk.

Historically, surgical manipulations of amphibian eye primordia have shown that correct placement of the OC within the head is crucial for signaling interactions with surrounding tissues (70–72). Particularly notable is the formation of a secondary NR upon rotation of the frog OC so that its presumptive RPE faced the surface ectoderm (71), a phenomenon that we also observed in AP-2α KO eyes. In the present study, we have examined in a genetic system how morphogenetic alterations in the developing OV/OC affect inductive interactions with adjacent tissues. Current models suggest that whereas cells in both the OV and presumptive lens ectoderm are biased toward particular identities before coming into contact, reciprocal signals direct further development of these two tissues (4,10,73). As they invaginate, the lens placode and OV are also physically connected by cytoplasmic processes recently identified as filopodia (74,75). We observed a mispositioning of the AP-2α KO OV at E9.5, in which it failed to fully contact the overlying ectoderm, permitting an accumulation of mesenchyme between the distal OV and surface ectoderm (Figs 2 and 3). This observation, combined with the fact that an obvious lens did not form in ∼25% of eyes, confirms that the interaction between the OV and surface ectoderm was disrupted spatially and/or temporally in AP-2α KO eyes. It is important to note that in conditional *Tcfap2a* KOs with deletion of *Tcfap2a* specifically from the lens, formation of a lens still occurs in 100% of eyes. Although these mutants exhibit a lens separation defect, their lenses are less dysmorphic than those of *Tcfap2a* germ-line KOs (32). Thus, deficient contact of the OV with the surface ectoderm is likely responsible for the increased severity of lens defects (or complete lack of a lens) observed in the germ-line KOs. This further supports the idea that multiple aspects of eye development in AP-2α germ-line KOs are affected in a non-cell autonomous fashion. Given that the OV is an extension of the neural tube, eye defects are commonly associated with neural tube defects, including split face and exencephaly (76,77) which are fully penetrant features of the AP-2α KO phenotype. The optic pits (future OVs) arise in the anterior neural plate before neural tube formation, therefore neurulation and OV evagination are intimately linked both temporally

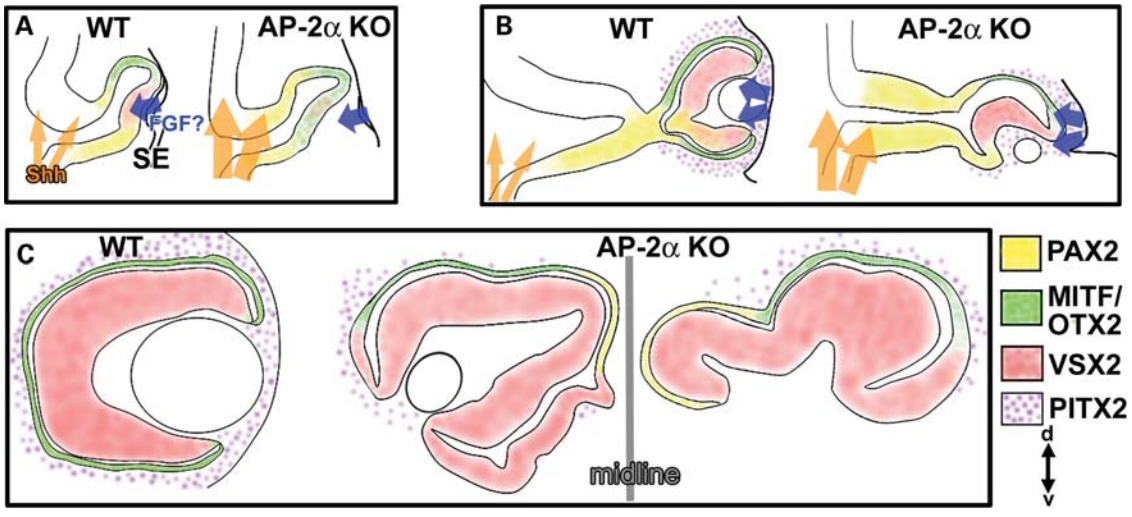

Figure 10. Summary of ocular neuroepithelium development in AP-2α germ-line KOs. All representative eyes depict coronal sections oriented according to the dorsal (d)–ventral (v) axis at bottom right. (**A**) At the OV stage, the forebrain neuroepithelium exhibits increased responsiveness to SHH, suggestive of increased activation of the SHH pathway (orange arrows). Deficient contact between the OV and surface ectoderm in AP-2α KOs disrupts lens formation and causes a persistence of RPE determinants (green) in the presumptive NR, likely due to the fact the distal OV is not close enough to NR-promoting signals from the surface ectoderm (possibly FGF; blue arrows). (**B**) The AP-2α KO OC typically develops in a position that is rotated to bring a portion of the dorsal presumptive RPE in apposition to the surface ectoderm. This rotation causes a segment of dorsal RPE to be transiently exposed to surface ectoderm-derived signals, which favors NR characteristics (red). As a result of failed optic stalk extension, the OC is pulled towards the midline, a source of SHH signals that presumably maintain PAX2 expression (yellow) in the proximal OC. The AP-2α KO eyes are also mispositioned with respect to PITX2-positive POM cells (stippled, purple), which further affects exposure to inductive signals. (**C**) The resulting AP-2α KO OCs sit adjacent to the midline and display variable defects, including lack of ventral retina tissue or a duplicated NR throughout the ventral RPE domain, regions of dorsal RPE-to-NR conversion and no optic stalk.

and spatially (78). The patterning and morphogenetic movements of progenitors in the neural plate, including cells in the retina field, are influenced by signals from neighboring tissues (1). In the AP-2α germ-line KOs, early loss of *Tcfap2a* from the neural folds and adjacent non-neural ectoderm may affect prospective OV cells in the neural plate so that their evagination from the neural tube is impaired. Subsequently, deficient contact of the OV with the surface ectoderm further exacerbates the overall eye phenotype.

The AP-2α KO optic neuroepithelium is not exposed to the correct developmental signals

Our data support the hypothesis that the developing eyes of AP-2α KO mice are exposed to inappropriate signaling interactions, causing major alterations in RPE and optic stalk cell fate (Fig. 10). Signals from the surface ectoderm, POM and forebrain have all been shown to impact patterning of the optic neuroepithelium (4,5,18), including midline-derived SHH (8,9). Patterning of the optic neuroepithelium along the proximal-distal axis (Fig. 1) is regulated by SHH signaling from the ventral midline, which promotes optic stalk specification through expression of *Pax2* and *Vax* genes, and establishes the optic stalk-OC boundary through suppression of retinal genes including *Pax6* (7–9). We detected evidence of increased SHH signaling in the AP-2α KO forebrain and OVs (Fig. 8), which likely contributed to multiple aspects of the ocular phenotype, including the ectopic PAX2 expression in the proximal OC. Indeed, overexpression of *Shh* in zebrafish and chick embryos results in microphthalmic eyes with expansion of the PAX2 expression domain (7,9). Notably, various mouse models with loss-of-function mutations in negative regulators of the SHH pathway (*Ptc*, *Rab23*, *Tulp3*) exhibit open neural tubes with expansion of ventral patterning markers (58,59,79,80). Increased midline SHH signaling also causes the ocular degeneration that has evolved among populations of blind cavefish (81). Although there are no previous reports suggesting involvement of AP-2 in the SHH pathway, the results presented here have provided an interesting avenue for further study.

Figure 10 summarizes the development of OC and optic stalk defects in AP-2α KOs. During early eye morphogenesis (Fig. 10A), the OVs do not correctly contact the surface ectoderm, resulting in abolished or defective lens formation and delayed patterning of the NR domain. This persistence of RPE determinants (MITF, OTX2) in the presumptive NR is likely due to the fact the distal OV is not close enough to NR-promoting signals from the surface ectoderm. The optic neuroepithelium is exposed to increased midline SHH signaling, resulting in ectopic PAX2 expression in the developing OC. As the OC forms in AP-2α KOs (Fig. 10B), it typically develops in a position that is rotated to bring a portion of the dorsal OC in apposition to the surface ectoderm. The OC rotation is presumably associated with the mispositioned lens rudiment. We hypothesize that this turning causes a segment of the outer OC to be transiently exposed to surface ectoderm-derived signals, such as FGF (10,12), which downregulate the expression of RPE-specifying genes and favor NR formation. Indeed, regions of the AP-2α KO dorsal OC that were turned towards the surface ectoderm were much more likely to exhibit NR characteristics.

As OC development progresses in AP-2α KOs, the optic stalk does not elongate and the eyes are gradually drawn towards the midline, which presumably maintains PAX2

expression in the proximal OC (Fig. 10B and C). Additional AP-2α KO ocular defects include failed optic fissure closure, and a variable ventral retina phenotype involving coloboma and total absence of RPE formation. Signals from the POM that are involved in RPE specification/maintenance or optic stalk morphogenesis, such as those regulated by PITX2, may be perturbed in the AP-2α KOs (Fig. 10B and C). A complete lack of optic stalk extension appears to be a relatively uncommon feature of mutant models. Nonetheless, this phenotype has been reported in mice lacking either *Pitx2* or all three retinoic acid receptors (RARs) specifically in the neural crest (15,82). In these mutants, as well as AP-2α KOs, PAX2 expression in the early optic stalk indicates that initial specification occurs; however, subsequent morphogenesis of the optic stalk is impaired (15,82). Recent studies have proposed a genetic cascade in the POM involving control of *Pitx2* expression by RA signaling (17,82). Importantly, we observed that AP-2α KO OCs were not surrounded by PITX2-positive POM cells to the same extent as controls, and noted a putative reduction in PITX2 protein in the POM of AP-2α KOs at E12.5 (Fig. 8), which may have contributed to some of the ocular defects, particularly the lack of optic stalk extension. Investigating a connection between AP-2α and RA/PITX2-related eye development will be important in future studies.

We also detected altered patterns of proliferation and apoptosis in AP-2α KO eyes (Fig. 9), although these changes were observed in non-AP-2α expressing cells and thus cannot be linked to cell autonomous loss of *Tcfap2a*. Although the exact roles of programmed cell death in development of the optic neuroepithelium are poorly understood, apoptosis has been linked to various morphogenetic events including OC invagination, optic fissure formation and invasion of optic fibers into the developing optic nerve (63,66,83). In AP-2α KOs, the lack of characteristic apoptotic regions in the early invaginating OC and developing optic stalk likely contributed to the gross morphological defects in these tissues, whereas the increased apoptosis observed in a proportion of later OCs may have contributed to the microphthalmia often observed in AP-2α KO mice.

AP-2α KO mice as a model for ocular defects in BOFS

The human AP-2α gene (*TFAP2A*), mapped to chromosome 6p24.2, has been implicated in 6p deletion syndromes (84–86), and most recently, BOFS (23–26), a genetic disorder characterized by craniofacial, oral, ear and eye anomalies. Our study provides insight into BOFS-related ocular defects, which are highly reflective of those in AP-2α KO mice. Eye defects in BOFS patients include anophthalmia, microphthalmia, primary aphakia (absence of the lens), cataractous and/or mispositioned lenses, other anterior segment defects, coloboma of the iris, retina or optic nerve and eyelid defects (23,25–28). Genetic screening has revealed a spectrum of *TFAP2A* mutations in BOFS cases, including deletions, insertions and missense mutations affecting conserved amino acids in the DNA binding domain, as well as large deletions encompassing the entire *TFAP2A* gene (23–26). Our ocular analysis of AP-2α KOs has highlighted the importance of precisely timed tissue–tissue interactions in the developing eye. Although each embryo contains the same loss of function mutation in a single gene, slight differences in these interactions, due to stochastic events during embryogenesis or subtle differences in the maternal environment, are likely factors contributing to the variability among AP-2α KO eye phenotypes. Accordingly, eye defects in BOFS cases are extremely variable, even among family members carrying identical *TFAP2A* mutations (26). Genetic modifiers may also account for the striking variations among human patients, which has recently been supported by a zebrafish study showing that morpholino knockdown of *tfap2a* in embryos already containing another mutation (in a component of the BMP or Wnt signaling pathways) exacerbates the eye defects caused by *tfap2a* knockdown alone (26).

In this study, we have characterized defects in derivatives of the AP-2α KO optic neuroepithelium. Given that tissue-specific deletion of *Tcfap2a* in the surface ectoderm, neural crest or retina does not recapitulate the AP-2α KO eye phenotype, the ocular defects in AP-2α KO mice must be caused by abnormalities in multiple tissues that contribute to the developing eye. Future studies may involve *Tcfap2a* deletion using a Cre transgenic line that targets AP-2α-expressing cells at the neural plate stage, or conditional *Tcfap2a* deletion using multiple Cre lines simultaneously (e.g. neural crest-specific and surface ectoderm-specific) in order to confirm the tissues through which AP-2α exerts its most crucial ocular morphogenetic roles. The ocular phenotypes of both mice and humans deficient in AP-2α demonstrate the importance of eye anomalies in the context of overall craniofacial development. Modifying signaling pathways known to impact craniofacial and/or ocular morphogenesis in the AP-2α germ-line KO background (e.g. Shh or Wnt) may provide further information regarding the factors involved in AP-2α-deficient eye and face development.

MATERIALS AND METHODS

Generation of AP-2α germ-line KO mice

All animal procedures were performed in accordance with the Association for Research in Vision and Ophthalmology (ARVO) Statement for the Use of Animals in Ophthalmic and Vision Research. Crosses were performed with mice on a mixed C57/Bl6 and FVB/N background. To generate AP-2α germ-line KOs, mice heterozygous for the *Tcfap2a*:*LacZ* KI null allele [due to a germ-line *lacZ* knock-in insertion disrupting exon 7 (69); $Tcfap2a^{ki7lacZ/+}$] were mated. Noon on the day of vaginal plug detection was considered day 0.5 (E0.5) of embryogenesis, and embryos were harvested immediately following euthanization of the pregnant female by CO_2 overdose. DNA was extracted from embryonic tail or yolk sac samples and ear clips of adult breeders using the DNeasy tissue kit (Qiagen). Mouse genotypes were determined by well established and previously reported PCR protocols (69). To detect the $Tcfap2a^{ki7lacZ}$ allele, PCR genotyping was performed using the forward primer Alpha 6/7 (5′-GAA AGG TGT AGG CAG AAG TTT GTC AGG GC-3′) and reverse primers Alpha3′KO (5′-CGT GTG GCT GTT GGG GTT GTT GCT GAG GTA C-3′) and IRESUP (5′-GCT AGA CTA GTC TAG CTA GAG CGG CCC GGG-3′) for

35 cycles (45 s at 95°C, 45 s at 70°C and 1 min at 72°C), generating a 500 bp wild-type (*Tcfap2a*$^{+}$) product and a 300 bp *Tcfap2a*^{ki7lacZ} product. Mutants were homozygous for the *Tcfap2a*^{ki7lacZ} null allele (*Tcfap2a*$^{ki7lacZ/ki7lacZ}$), and littermates used as controls were homozygous for the wild-type *Tcfap2a*$^{+}$ allele (*Tcfap2a*$^{+/+}$).

Histology

Dissected embryos were fixed in 10% neutral buffered formalin (Sigma-Aldrich, Oakville, ON, Canada) overnight at room temperature, processed and embedded in paraffin wax. Serial sections were cut 4 μm in thickness and used for haematoxylin and eosin (H&E) staining, immunofluorescent analysis or the TUNEL assay. For all stages examined, a minimum of six eyes were stained for each genotype (control or mutant).

In situ hybridization, immunofluorescence and tunel assay

Whole mount *in situ* hybridization using digoxygenin-labeled riboprobe for Gli1 was performed as previously described (87,88) with the following modifications: Pre-hybridizing and hybridizing buffer contained 4xSSC and post-hybridization washes were conducted in buffer with 2xSSC. Indirect immunofluorescence was performed using the following primary antibodies: rabbit polyclonal anti-Islet1/2 (K5) at 1:500 (Dr Thomas Jessell lab, Columbia University, New York, NY, USA); rabbit polyclonal anti-PH3 at 1:100 (Upstate, Charlottesville, VA, USA); rabbit polyclonal anti-Otx2 (Abcam) at 1:100; rabbit polyclonal anti-Pax6 (Covance, Princeton, NJ, USA) at 1:50; mouse monoclonal anti-Mitf at 1:200 (Lab Vision/NeoMarkers, Fremont, CA, USA); sheep polyclonal anti-Vsx2/Chx10 at 1:40 (Exalpha Biologicals, Inc., Watertown, MA, USA); rabbit polyclonal anti-Pax2 at 1:100 (Zymed, Carlsbad, CA, USA); mouse monoclonal anti-β-tubulin isotype III clone SDL.3D10 at 1:1000 (Sigma-Aldrich, Oakville, ON, Canada); rabbit polyclonal anti-Pitx2 (gift from T. Hjalt). Fluorescent secondary antibodies were Alexa Flour 488 or 568 (Invitrogen—Molecular Probes, Burlington, ON, Canada) used 1:200 for 1 h at room temperature. For all primary antibodies except anti-Mitf, paraffin-embedded sections were deparaffinized in xylene, hydrated (through 100, 95 and 70% ethanol, followed by water), treated for antigen retrieval with 10 mM sodium citrate buffer pH 6.0, boiling for 20 min, blocked with normal serum and incubated with primary antibodies overnight at 4°C. Immunostaining with the Mitf antibody utilized the above protocol with two modifications: antigen retrieval in 1 mM EDTA pH 8.0, and incubation with the primary antibody for 1 h at room temperature. For the Pax2/Mitf co-immunostain, both primaries and both secondaries were mixed and incubated simultaneously, using the anti-Mitf procedure. Terminal uridine deoxynucleotidyl transferase-mediated dUTP Nick End Labeling (TUNEL) was performed using the ApopTag® Plus Fluorescein *In Situ* Apoptosis Detection Kit (Millipore-Chemicon, Billerica, MA, USA), according to the manufacturer's instructions for fluorescent staining of paraffin-embedded tissue. Following immunofluorescence or the TUNEL assay, stains were mounted with Vectashield mounting medium containing 4,6-diamino-2-phenylindole (DAPI; Vector Laboratories, Burlington, ON, Canada). All stains were visualized with a microscope (Leica, Deerfield, IL, USA) equipped with a fluorescence attachment, and images were captured with a high-resolution camera and associated software (Open-Lab; Improvision, Lexington, MA, USA). Images were reproduced for publication with image-management software (Photoshop 7.0; Adobe Systems Inc., Mountain View, CA, USA).

SUPPLEMENTARY MATERIAL

Supplementary Material is available at *HMG* online.

ACKNOWLEDGEMENTS

We thank Sanghee Yun, Dr Ed Levine and Dr Valerie Wallace for providing the Gli1 *in situ* probe, and Andrew Loudon for technical assistance.

Conflict of Interest statement. None declared.

FUNDING

This work was supported by the National Eye Institute/National Institutes of Health (EY01426, EY007003 to P.J.G., EY11910 to J.W.-M., EY014954, Core Grant EY014800 to S.F.); National Institute of Dental and Craniofacial Research/National Institutes of Health (DE-12728 to T.W.); and Research to Prevent Blindness to J.W.-M. and to the Department of Ophthalmology, University of Utah.

REFERENCES

1. Wilson, S.W. and Houart, C. (2004) Early steps in the development of the forebrain. *Dev. Cell*, **6**, 167–181.
2. Rubenstein, J.L. and Beachy, P.A. (1998) Patterning of the embryonic forebrain. *Curr. Opin. Neurobiol.*, **8**, 18–26.
3. Gage, P.J., Rhoades, W., Prucka, S.K. and Hjalt, T. (2005) Fate maps of neural crest and mesoderm in the mammalian eye. *Invest. Ophthalmol. Vis. Sci.*, **46**, 4200–4208.
4. Chow, R.L. and Lang, R.A. (2001) Early eye development in vertebrates. *Annu. Rev. Cell. Dev. Biol.*, **17**, 255–296.
5. Yang, X.J. (2004) Roles of cell-extrinsic growth factors in vertebrate eye pattern formation and retinogenesis. *Semin. Cell Dev. Biol.*, **15**, 91–103.
6. Huh, S., Hatini, V., Marcus, R.C., Li, S.C. and Lai, E. (1999) Dorsal-ventral patterning defects in the eye of BF-1-deficient mice associated with a restricted loss of shh expression. *Dev. Biol.*, **211**, 53–63.
7. Macdonald, R., Barth, K.A., Xu, Q., Holder, N., Mikkola, I. and Wilson, S.W. (1995) Midline signalling is required for Pax gene regulation and patterning of the eyes. *Development*, **121**, 3267–3278.
8. Take-uchi, M., Clarke, J.D. and Wilson, S.W. (2003) Hedgehog signalling maintains the optic stalk-retinal interface through the regulation of Vax gene activity. *Development*, **130**, 955–968.
9. Zhang, X.M. and Yang, X.J. (2001) Temporal and spatial effects of Sonic hedgehog signaling in chick eye morphogenesis. *Dev. Biol.*, **233**, 271–290.
10. Horsford, D.J., Nguyen, M.T., Sellar, G.C., Kothary, R., Arnheiter, H. and McInnes, R.R. (2005) Chx10 repression of Mitf is required for the maintenance of mammalian neuroretinal identity. *Development*, **132**, 177–187.
11. Hyer, J., Mima, T. and Mikawa, T. (1998) FGF1 patterns the optic vesicle by directing the placement of the neural retina domain. *Development*, **125**, 869–877.

12. Nguyen, M. and Arnheiter, H. (2000) Signaling and transcriptional regulation in early mammalian eye development: a link between FGF and MITF. *Development*, **127**, 3581–3591.
13. Fuhrmann, S., Levine, E.M. and Reh, T.A. (2000) Extraocular mesenchyme patterns the optic vesicle during early eye development in the embryonic chick. *Development*, **127**, 4599–4609.
14. Berry, F.B., Lines, M.A., Oas, J.M., Footz, T., Underhill, D.A., Gage, P.J. and Walter, M.A. (2006) Functional interactions between FOXC1 and PITX2 underlie the sensitivity to FOXC1 gene dose in Axenfeld-Rieger syndrome and anterior segment dysgenesis. *Hum. Mol. Genet.*, **15**, 905–919.
15. Evans, A.L. and Gage, P.J. (2005) Expression of the homeobox gene Pitx2 in neural crest is required for optic stalk and ocular anterior segment development. *Hum. Mol. Genet.*, **14**, 3347–3359.
16. Cvekl, A. and Tamm, E.R. (2004) Anterior eye development and ocular mesenchyme: new insights from mouse models and human diseases. *Bioessays*, **26**, 374–386.
17. Gage, P.J. and Zacharias, A.L. (2009) Signaling 'cross-talk' is integrated by transcription factors in the development of the anterior segment in the eye. *Dev. Dyn.*, **238**, 2149–2162.
18. Adler, R. and Canto-Soler, M.V. (2007) Molecular mechanisms of optic vesicle development: complexities, ambiguities and controversies. *Dev. Biol.*, **305**, 1–13.
19. Bharti, K., Nguyen, M.T., Skuntz, S., Bertuzzi, S. and Arnheiter, H. (2006) The other pigment cell: specification and development of the pigmented epithelium of the vertebrate eye. *Pigment Cell Res.*, **19**, 380–394.
20. Fujimura, N., Taketo, M.M., Mori, M., Korinek, V. and Kozmik, Z. (2009) Spatial and temporal regulation of Wnt/beta-catenin signaling is essential for development of the retinal pigment epithelium. *Dev. Biol.*, **334**, 31–45.
21. Martinez-Morales, J.R., Rodrigo, I. and Bovolenta, P. (2004) Eye development: a view from the retina pigmented epithelium. *Bioessays*, **26**, 766–777.
22. Westenskow, P., Piccolo, S. and Fuhrmann, S. (2009) {beta}-catenin controls differentiation of the retinal pigment epithelium in the mouse optic cup by regulating Mitf and Otx2 expression. *Development*, **136**, 2505–2510.
23. Stoetzel, C., Riehm, S., Bennouna Greene, V., Pelletier, V., Vigneron, J., Leheup, B., Marion, V., Helle, S., Danse, J.M., Thibault, C. *et al.* (2009) Confirmation of TFAP2A gene involvement in branchio-oculo-facial syndrome (BOFS) and report of temporal bone anomalies. *Am. J. Med. Genet. A*, **149A**, 2141–2146.
24. Tekin, M., Sirmaci, A., Yuksel-Konuk, B., Fitoz, S. and Sennaroglu, L. (2009) A complex TFAP2A allele is associated with branchio-oculo-facial syndrome and inner ear malformation in a deaf child. *Am. J. Med. Genet. A*, **149A**, 427–430.
25. Milunsky, J.M., Maher, T.A., Zhao, G., Roberts, A.E., Stalker, H.J., Zori, R.T., Burch, M.N., Clemens, M., Mulliken, J.B., Smith, R. *et al.* (2008) TFAP2A mutations result in branchio-oculo-facial syndrome. *Am. J. Hum. Genet.*, **82**, 1171–1177.
26. Gestri, G., Osborne, R.J., Wyatt, A.W., Gerrelli, D., Gribble, S., Stewart, H., Fryer, A., Bunyan, D.J., Prescott, K., Collin, J.R. *et al.* (2009) Reduced TFAP2A function causes variable optic fissure closure and retinal defects and sensitizes eye development to mutations in other morphogenetic regulators. *Hum. Genet.*, **126**, 719–803.
27. Lin, A.E., Losken, H.W., Jaffe, R. and Biglan, A.W. (1991) The branchio-oculo-facial syndrome. *Cleft Palate Craniofac. J.*, **28**, 96–102.
28. Lin, A.E., Gorlin, R.J., Lurie, I.W., Brunner, H.G., van der Burgt, I., Naumchik, I.V., Rumyantseva, N.V., Stengel-Rutkowski, S., Rosenbaum, K., Meinecke, P. *et al.* (1995) Further delineation of the branchio-oculo-facial syndrome. *Am. J. Med. Genet.*, **56**, 42–59.
29. West-Mays, J.A., Zhang, J., Nottoli, T., Hagopian-Donaldson, S., Libby, D., Strissel, K.J. and Williams, T. (1999) AP-2alpha transcription factor is required for early morphogenesis of the lens vesicle. *Dev. Biol.*, **206**, 46–62.
30. West-Mays, J.A., Coyle, B.M., Piatigorsky, J., Papagiotas, S. and Libby, D. (2002) Ectopic expression of AP-2alpha transcription factor in the lens disrupts fiber cell differentiation. *Dev. Biol.*, **245**, 13–27.
31. West-Mays, J.A., Sivak, J.M., Papagiotas, S.S., Kim, J., Nottoli, T., Williams, T. and Fini, M.E. (2003) Positive influence of AP-2alpha transcription factor on cadherin gene expression and differentiation of the ocular surface. *Differentiation*, **71**, 206–216.
32. Pontoriero, G.F., Deschamps, P., Ashery-Padan, R., Wong, R., Yang, Y., Zavadil, J., Cvekl, A., Sullivan, S., Williams, T. and West-Mays, J.A. (2008) Cell autonomous roles for AP-2alpha in lens vesicle separation and maintenance of the lens epithelial cell phenotype. *Dev. Dyn.*, **237**, 602–617.
33. Dwivedi, D.J., Pontoriero, G.F., Ashery-Padan, R., Sullivan, S., Williams, T. and West-Mays, J.A. (2005) Targeted deletion of AP-2alpha leads to disruption in corneal epithelial cell integrity and defects in the corneal stroma. *Invest. Ophthalmol. Vis. Sci.*, **46**, 3623–3630.
34. Bassett, E.A., Pontoriero, G.F., Feng, W., Marquardt, T., Fini, M.E., Williams, T. and West-Mays, J.A. (2007) Conditional deletion of activating protein 2alpha (AP-2alpha) in the developing retina demonstrates non-cell-autonomous roles for AP-2alpha in optic cup development. *Mol. Cell. Biol.*, **27**, 7497–7510.
35. Mitchell, P.J., Timmons, P.M., Hebert, J.M., Rigby, P.W. and Tjian, R. (1991) Transcription factor AP-2 is expressed in neural crest cell lineages during mouse embryogenesis. *Genes Dev.*, **5**, 105–119.
36. Moser, M., Ruschoff, J. and Buettner, R. (1997) Comparative analysis of AP-2 alpha and AP-2 beta gene expression during murine embryogenesis. *Dev. Dyn.*, **208**, 115–124.
37. Schorle, H., Meier, P., Buchert, M., Jaenisch, R. and Mitchell, P.J. (1996) Transcription factor AP-2 essential for cranial closure and craniofacial development. *Nature*, **381**, 235–238.
38. Zhang, J., Hagopian-Donaldson, S., Serbedzija, G., Elsemore, J., Plehn-Dujowich, D., McMahon, A.P., Flavell, R.A. and Williams, T. (1996) Neural tube, skeletal and body wall defects in mice lacking transcription factor AP-2. *Nature*, **381**, 238–241.
39. Bora, N., Conway, S.J., Liang, H. and Smith, S.B. (1998) Transient overexpression of the Microphthalmia gene in the eyes of Microphthalmia vitiligo mutant mice. *Dev. Dyn.*, **213**, 283–292.
40. Burmeister, M., Novak, J., Liang, M.Y., Basu, S., Ploder, L., Hawes, N.L., Vidgen, D., Hoover, F., Goldman, D., Kalnins, V.I. *et al.* (1996) Ocular retardation mouse caused by Chx10 homeobox null allele: impaired retinal progenitor proliferation and bipolar cell differentiation. *Nat. Genet.*, **12**, 376–384.
41. Liu, I.S., Chen, J.D., Ploder, L., Vidgen, D., van der Kooy, D., Kalnins, V.I. and McInnes, R.R. (1994) Developmental expression of a novel murine homeobox gene (Chx10): evidence for roles in determination of the neuroretina and inner nuclear layer. *Neuron*, **13**, 377–393.
42. Martinez-Morales, J.R., Signore, M., Acampora, D., Simeone, A. and Bovolenta, P. (2001) Otx genes are required for tissue specification in the developing eye. *Development*, **128**, 2019–2030.
43. Galli-Resta, L., Resta, G., Tan, S.S. and Reese, B.E. (1997) Mosaics of islet-1-expressing amacrine cells assembled by short-range cellular interactions. *J. Neurosci.*, **17**, 7831–7838.
44. Pak, W., Hindges, R., Lim, Y.S., Pfaff, S.L. and O'Leary, D.D. (2004) Magnitude of binocular vision controlled by islet-2 repression of a genetic program that specifies laterality of retinal axon pathfinding. *Cell*, **119**, 567–578.
45. Koike, C., Nishida, A., Ueno, S., Saito, H., Sanuki, R., Sato, S., Furukawa, A., Aizawa, S., Matsuo, I., Suzuki, N. *et al.* (2007) Functional roles of Otx2 transcription factor in postnatal mouse retinal development. *Mol. Cell. Biol.*, **27**, 8318–8329.
46. Baas, D., Bumsted, K.M., Martinez, J.A., Vaccarino, F.M., Wikler, K.C. and Barnstable, C.J. (2000) The subcellular localization of Otx2 is cell-type specific and developmentally regulated in the mouse retina. *Brain Res. Mol. Brain Res.*, **78**, 26–37.
47. Nishida, A., Furukawa, A., Koike, C., Tano, Y., Aizawa, S., Matsuo, I. and Furukawa, T. (2003) Otx2 homeobox gene controls retinal photoreceptor cell fate and pineal gland development. *Nat. Neurosci.*, **6**, 1255–1263.
48. Schwarz, M., Cecconi, F., Bernier, G., Andrejewski, N., Kammandel, B., Wagner, M. and Gruss, P. (2000) Spatial specification of mammalian eye territories by reciprocal transcriptional repression of Pax2 and Pax6. *Development*, **127**, 4325–4334.
49. Nornes, H.O., Dressler, G.R., Knapik, E.W., Deutsch, U. and Gruss, P. (1990) Spatially and temporally restricted expression of Pax2 during murine neurogenesis. *Development*, **109**, 797–809.
50. Torres, M., Gomez-Pardo, E. and Gruss, P. (1996) Pax2 contributes to inner ear patterning and optic nerve trajectory. *Development*, **122**, 3381–3391.

51. Otteson, D.C., Shelden, E., Jones, J.M., Kameoka, J. and Hitchcock, P.F. (1998) Pax2 expression and retinal morphogenesis in the normal and Krd mouse. *Dev. Biol.*, **193**, 209–224.
52. Hero, I. (1990) Optic fissure closure in the normal cinnamon mouse. An ultrastructural study. *Invest. Ophthalmol. Vis. Sci.*, **31**, 197–216.
53. Bai, C.B., Auerbach, W., Lee, J.S., Stephen, D. and Joyner, A.L. (2002) Gli2, but not Gli1, is required for initial Shh signaling and ectopic activation of the Shh pathway. *Development*, **129**, 4753–4761.
54. Sigulinsky, C.L., Green, E.S., Clark, A.M. and Levine, E.M. (2008) Vsx2/Chx10 ensures the correct timing and magnitude of Hedgehog signaling in the mouse retina. *Dev. Biol.*, **317**, 560–575.
55. Furimsky, M. and Wallace, V.A. (2006) Complementary Gli activity mediates early patterning of the mouse visual system. *Dev. Dyn.*, **235**, 594–605.
56. Hui, C.C., Slusarski, D., Platt, K.A., Holmgren, R. and Joyner, A.L. (1994) Expression of three mouse homologs of the Drosophila segment polarity gene cubitus interruptus, Gli, Gli-2 and Gli-3, in ectoderm- and mesoderm-derived tissues suggests multiple roles during postimplantation development. *Dev. Biol.*, **162**, 402–413.
57. Ericson, J., Muhr, J., Placzek, M., Lints, T., Jessell, T.M. and Edlund, T. (1995) Sonic hedgehog induces the differentiation of ventral forebrain neurons: a common signal for ventral patterning within the neural tube. *Cell*, **81**, 747–756.
58. Patterson, V.L., Damrau, C., Paudyal, A., Reeve, B., Grimes, D.T., Stewart, M.E., Williams, D.J., Siggers, P., Greenfield, A. and Murdoch, J.N. (2009) Mouse hitchhiker mutants have spina bifida, dorso-ventral patterning defects and polydactyly: identification of Tulp3 as a novel negative regulator of the Sonic hedgehog pathway. *Hum. Mol. Genet.*, **18**, 1719–1739.
59. Eggenschwiler, J.T. and Anderson, K.V. (2000) Dorsal and lateral fates in the mouse neural tube require the cell-autonomous activity of the open brain gene. *Dev. Biol.*, **227**, 648–660.
60. Ericson, J., Muhr, J., Jessell, T.M. and Edlund, T. (1995) Sonic hedgehog: a common signal for ventral patterning along the rostrocaudal axis of the neural tube. *Int. J. Dev. Biol.*, **39**, 809–816.
61. Gage, P.J., Suh, H. and Camper, S.A. (1999) Dosage requirement of Pitx2 for development of multiple organs. *Development*, **126**, 4643–4651.
62. Sowden, J.C. (2007) Molecular and developmental mechanisms of anterior segment dysgenesis. *Eye*, **21**, 1310–1318.
63. Silver, J. and Hughes, A.F. (1973) The role of cell death during morphogenesis of the mammalian eye. *J. Morphol.*, **140**, 159–170.
64. Laemle, L.K., Puszkarczuk, M. and Feinberg, R.N. (1999) Apoptosis in early ocular morphogenesis in the mouse. *Brain Res. Dev. Brain Res.*, **112**, 129–133.
65. Lang, R.A. (1997) Apoptosis in mammalian eye development: lens morphogenesis, vascular regression and immune privilege. *Cell Death Differ.*, **4**, 12–20.
66. Silver, J. and Robb, R.M. (1979) Studies on the development of the eye cup and optic nerve in normal mice and in mutants with congenital optic nerve aplasia. *Dev. Biol.*, **68**, 175–190.
67. Serbedzija, G.N., Bronner-Fraser, M. and Fraser, S.E. (1992) Vital dye analysis of cranial neural crest cell migration in the mouse embryo. *Development*, **116**, 297–307.
68. Brewer, S., Feng, W., Huang, J., Sullivan, S. and Williams, T. (2004) Wnt1-Cre-mediated deletion of AP-2alpha causes multiple neural crest-related defects. *Dev. Biol.*, **267**, 135–152.
69. Brewer, S., Jiang, X., Donaldson, S., Williams, T. and Sucov, H.M. (2002) Requirement for AP-2alpha in cardiac outflow tract morphogenesis. *Mech. Dev.*, **110**, 139–149.
70. Detwiler, S.R. and van Dyke, R.H. (1953) The induction of neural retina from the pigment epithelial layer of the eye. *J. Exp. Zool.*, **122**, 367–383.
71. Dragomirov, N. (1937) The influence of neighboring ectoderm on the organization of eye rudiment. *Dokl. Akad. Nauk SSSR*, **15**, 61–64.
72. Lopashov, G.V. and Stroeva, O.G. (1964) *Development of the Eye: Experimental Studies*, Davey & Co, New York.
73. Donner, A.L., Lachke, S.A. and Maas, R.L. (2006) Lens induction in vertebrates: variations on a conserved theme of signaling events. *Semin. Cell Dev. Biol.*, **17**, 676–685.
74. Chauhan, B.K., Disanza, A., Choi, S.Y., Faber, S.C., Lou, M., Beggs, H.E., Scita, G., Zheng, Y. and Lang, R.A. (2009) Cdc42- and IRSp53-dependent contractile filopodia tether presumptive lens and retina to coordinate epithelial invagination. *Development*, **136**, 3657–3667.
75. McAvoy, J.W. (1980) Cytoplasmic processes interconnect lens placode and optic vesicle during eye morphogenesis. *Exp. Eye Res.*, **31**, 527–534.
76. Harris, M.J. and Juriloff, D.M. (1999) Mini-review: toward understanding mechanisms of genetic neural tube defects in mice. *Teratology*, **60**, 292–305.
77. Harris, M.J. and Juriloff, D.M. (2007) Mouse mutants with neural tube closure defects and their role in understanding human neural tube defects. *Birth Defects Res. A Clin. Mol. Teratol.*, **79**, 187–210.
78. Kaufman, M. (1979) Cephalic neurulation and optic vesicle formation in the early mouse embryo. *Am. J. Anat.*, **155**, 425–443.
79. Milenkovic, L., Goodrich, L.V., Higgins, K.M. and Scott, M.P. (1999) Mouse patched1 controls body size determination and limb patterning. *Development*, **126**, 4431–4440.
80. Goodrich, L.V., Milenkovic, L., Higgins, K.M. and Scott, M.P. (1997) Altered neural cell fates and medulloblastoma in mouse patched mutants. *Science*, **277**, 1109–1113.
81. Yamamoto, Y., Stock, D.W. and Jeffery, W.R. (2004) Hedgehog signalling controls eye degeneration in blind cavefish. *Nature*, **431**, 844–847.
82. Matt, N., Ghyselinck, N.B., Pellerin, I. and Dupe, V. (2008) Impairing retinoic acid signalling in the neural crest cells is sufficient to alter entire eye morphogenesis. *Dev. Biol.*, **320**, 140–148.
83. Rodriguez-Gallardo, L., Lineros-Dominguez Mdel, C., Francisco-Morcillo, J. and Martin-Partido, G. (2005) Macrophages during retina and optic nerve development in the mouse embryo: relationship to cell death and optic fibres. *Anat. Embryol. (Berl).*, **210**, 303–316.
84. Davies, A.F., Mirza, G., Flinter, F. and Ragoussis, J. (1999) An interstitial deletion of 6p24-p25 proximal to the FKHL7 locus and including AP-2alpha that affects anterior eye chamber development. *J. Med. Genet.*, **36**, 708–710.
85. Davies, A.F., Mirza, G., Sekhon, G., Turnpenny, P., Leroy, F., Speleman, F., Law, C., van Regemorter, N., Vamos, E., Flinter, F. *et al.* (1999) Delineation of two distinct 6p deletion syndromes. *Hum. Genet.*, **104**, 64–72.
86. Moriarty, A.P. and Kerr-Muir, M.G. (1992) Sclerocornea and interstitial deletion of the short arm of chromosome 6-(46XY del[6] [p22 p24]). *J. Pediatr. Ophthalmol. Strabismus*, **29**, 177–179.
87. Burns, C.J., Zhang, J., Brown, E.C., Van Bibber, A.M., Van Es, J., Clevers, H., Ishikawa, T.O., Taketo, M.M., Vetter, M.L. and Fuhrmann, S. (2008) Investigation of Frizzled-5 during embryonic neural development in mouse. *Dev. Dyn.*, **237**, 1614–1626.
88. Henrique, D., Adam, J., Myat, A., Chitnis, A., Lewis, J. and Ish-Horowicz, D. (1995) Expression of a Delta homologue in prospective neurons in the chick. *Nature*, **375**, 787–790.